Analyst

PAPER

View Article Online
View Journal | View Issue



Cite this: *Analyst*, 2015, **140**, 6922

# Investigating carbohydrate isomers by IMS-CID-IMS-MS: precursor and fragment ion cross-sections

M. M. Gaye, R. Kurulugama† and D. E. Clemmer*

Ion mobility spectrometry techniques (IMS and IMS-IMS) combined with collision-induced dissociation (CID) and mass spectrometry (MS) are used to investigate the structures of singly-lithiated carbohydrate isomers. With the exception of some favorable cases, IMS-MS analyses of underivatized carbohydrates reveal that most isobaric precursor ions have similar collision cross sections (ccs). In contrast, ccs values for isomeric fragment ions obtained by IMS-CID-IMS-MS analysis are often different, and thus appear to be useful as a means of distinguishing the isomeric precursors. We report values of ccs (in He) for precursor- and associated-fragment ions for three monosaccharide isomers (glucose, galactose and fructose), ten disaccharide isomers (sucrose, leucrose, palatinose, trehalose, cellobiose, β-gentiobiose, isomaltose, maltose, lactose and melibiose), and three trisaccharide isomers (raffinose, melezitose and maltotriose). These values are discussed as a means of differentiating precursor carbohydrates.

Received 28th April 2015,
Accepted 7th August 2015

DOI: 10.1039/c5an00840a

www.rsc.org/analyst



## Introduction

High-throughput, structural characterization of carbohydrates is proving to be challenging. In part, this is because unlike linear chains of nucleic or amino acids (associated with DNA and protein sequences), carbohydrates may be made up from 20 common monosaccharide units that may be linked at five potential positions on each saccharide ring; additionally, there are two possible anomeric configurations of the linkages, some units have different ring sizes (*e.g.*, furanose has five carbons in its ring, while pyranose has six), and numerous modifications can occur on the monomeric unit (*e.g.*, sulfation and phosphorylation).[1,2] In addition to the intrinsic complexity, often only limited amounts of samples may exist (*i.e.*, a few μg, or less), and when available samples may be comprised of mixtures of closely related species such as isomers. In favorable cases, detailed three-dimensional geometric assignments of carbohydrate structures can be obtained by nuclear magnetic resonance (NMR) or crystallography.[3,4] However, NMR typically requires milligrams of samples, is of limited utility for mixture analysis, and is not suitable for high-throughput analyses; and, crystallography requires a crystal, either of the isolated carbohydrate or a crystalized region of the molecule as it interacts with a protein or other species that is also crystalized.[4]

Advances in ionization techniques have made it possible to investigate carbohydrate structures by a range of mass spectrometry (MS) and associated separation techniques. MS techniques are extremely sensitive, making it possible to carry out experiments with vanishingly small quantities. Moreover, these techniques are well-suited for mixture analysis and can be applied in a high-throughput fashion. In the present work, the structures of carbohydrate precursor and fragment ions are investigated by a combination of ion mobility spectrometry (IMS) and MS techniques. Because an ion's mobility depends on its shape, this combination of techniques is proving to be valuable for discerning between different isomeric forms.[5,6]

The studies presented below use collision-induced dissociation (CID) which allows us to use differences in fragment-ion structures to identify different disaccharide and trisaccharide isomers. We have chosen precursors comprised of a small number of monosaccharide units, and having an isomeric affiliation with one another. These are shown in Scheme 1. Sucrose, leucrose and palatinose are disaccharides of glucose and fructose, linked by an α-glycosidic bond. They differ only in linkage position (1–2, 1–5 and 1–6, respectively, where the first number indicates the position on the monosaccharide unit at the non-reducing end and the second number indicates the linkage position on the monosaccharide unit at the reducing end). Five other disaccharides (trehalose, cellobiose, β-gentiobiose, isomaltose and maltose) are comprised solely of

*Department of Chemistry, Indiana University, Bloomington, IN 47405, USA.*
*E-mail: clemmer@indiana.edu*
† Present address: Agilent Technologies, Santa Clara, CA 95501.

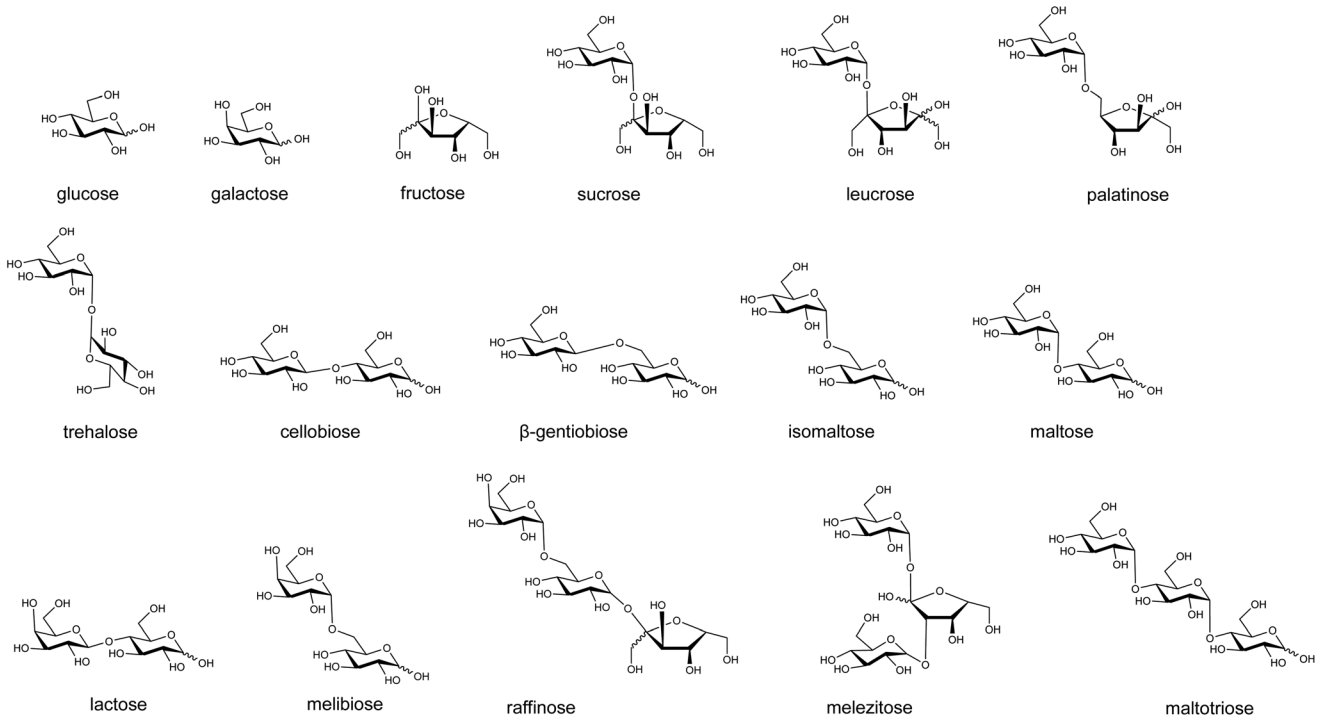


**Scheme 1** Structure of the studied carbohydrates.

glucose units. These differ by the linkage anomericity, linkage position, or both. Two additional disaccharides, lactose and melibiose are comprised of galactose and glucose monomer units and differ from one another by linkage position and anomericity. Raffinose, melizitose and maltotriose are trisaccharides comprised of glucose and/or galactose and/or fructose residues. Additionally, cross sections for the intact monomers of glucose, galactose, and fructose, are reported as well.

This work builds on prior work using condensed-phase separation techniques such as capillary electrophoresis (CE) or high pressure liquid chromatography (often following sequential exoglycosidase digestion) along with multi-stage mass spectrometry ($MS^n$) for the elucidation of carbohydrate isomeric structures.[7–10] Carbohydrate fragment ions can be produced by CID,[9,11,12] electron capture (or transfer) dissociation [ECD, (or ETD)],[13–16] and vacuum ultraviolet photodissociation (VUVPD).[17–19] Fragmentation *via* CID primarily occurs *via* glycosidic bond cleavage; ECD, ETD and VUVPD produce additional cross-ring fragments useful for linkage position information.[9,11–14,16–19] Often, multi-stage $MS^n$ is necessary because fragment ions after $MS^2$ may be isobaric[20] such that no specific structural information can be obtained. Although powerful algorithms have been developed to overcome this difficulty,[9,21] there is still a need for complementary technologies for carbohydrate analysis. Below, we explore IMS as a means of complementing MS-based structural assignments.

A number of recent studies have used IMS-MS techniques to investigate carbohydrate structures.[19,22–35] Early on, Liu *et al.*[22] established that isomeric fragment ions (originating from isomeric precursor ions) could be distinguished based on differences in mobilities through $N_2$ buffer gas. Lee *et al.* used a combination of IMS with VUVPD to characterize a mixture of seven disaccharides by using the extracted fragment drift time distributions of specific fragment ions that were unique to each disaccharide.[19] Finally, the present work is also closely related to elegant studies by Hill's[34] and Eyers's[36] groups, using different combinations of IMS-MS and CID methodologies. Overall, our efforts in combination with the studies conducted by Hill, Eyers, and coworkers,[34,36] are of significance towards the establishment of a ccs library of carbohydrate precursor and fragment ions, which in due course will lead to high-throughput sequencing capabilities for carbohydrates.

## Experimental section

### Materials and sample preparation

Thirteen carbohydrates (all in the D(+) form) were purchased from Sigma-Aldrich (St. Louis, MO). Three of these were the monosaccharides glucose, fructose and galactose; eight were the disaccharides sucrose, palatinose, leucrose, maltose, trehalose, lactose, cellobiose, and β-gentiobiose; and, two were the trisaccharides melezitose, and raffinose. The disaccharides, isomaltose and melibiose as well as the trisaccharide maltotriose were obtained from Santa Cruz Biotechnology (Dallas, TX). All carbohydrates were used directly as purchased. The

structures for all of these molecules are depicted in Scheme 1. Solutions for electrospray were prepared as 0.25 mg $ml^{-1}$ in a 90 : 10 (vol%) water : acetonitrile and 2.0 mM LiCl.

### IMS-MS and IMS-CID-IMS-MS measurements

Theoretical and experimental aspects of an IMS-MS measurement as well as the home-built IMS-time-of-flight (TOF) MS instrument used in this study are described elsewhere.[5,37–40] A schematic diagram of the instrument is shown in Fig. 1. The instrument consists of an electrospray ionization (ESI) source coupled with an automatic injection system (NanoMate TriVersa, Advion, Ithaca, NY), a two meter long drift tube (D1 and D2) that is equipped with an ion selection and activation region, and a TOF mass analyzer. In a typical IMS-MS experiment, ions are accumulated in the source ion funnel (F1) and periodically pulsed into the drift tube as a narrow packet of ions (150 μs wide), where they are separated according to their mobilities in He buffer gas. Ions exit the drift tube through a differentially pumped region and are extracted into the source region of a reflectron geometry TOF for mass analysis and detection. In the present experiment, the drift tube is filled with ~2.3 Torr of He at 294 K and operated under a uniform electric field of 9.6 V $cm^{-1}$. The source ion funnel is operated at 15 V $cm^{-1}$ and ~1.69 Torr of He; the back (F3, Fig. 1) and mid (F2, Fig. 1) ion funnels are operated at 12 V $cm^{-1}$ and ~2.25 Torr of He. A radio frequency field ranging from 390 to 440 kHz with a peak-to-peak amplitude of 120 to 140 $V_{p-p}$ is applied to all three ion funnels.

A unique feature of this instrumentation is the ability to select and activate mobility-separated ions. In an IMS-CID-IMS-MS experiment, the two parts of the drift tube D1 and D2 are operated independently. That is, a first pulse (G1, Fig. 1) introduces all ions in D1 and a synchronized second pulse (G2), applied at the entrance of the mid ion funnel, allows only a narrow distribution of ions with specified mobilities into F2. For all carbohydrates presented in Table 1 the precursor ion $[M + Li]^+$ is selected at the entrance of the second drift region, after ~72 cm of mobility separation. The mobility-selected ions are subsequently fragmented in the ion activation region (IA2, Fig. 1, comprised of two lenses which are spaced ~0.3 cm apart). The resulting fragments are mobility separated in the second drift tube, region D2 prior to mass analysis. Fragmentation studies are performed by raising the field across IA2 from 12 V $cm^{-1}$ to 530 V $cm^{-1}$ for disaccharides and from 12 V $cm^{-1}$ to 615 V $cm^{-1}$ for trisaccharides. IMS-CID-IMS-MS has been previously used in our group for the analysis of peptide and protein fragment ions.[41] We report here the application of this technique to the characterization of carbohydrate isomeric ions.

The IMS-CID-IMS-MS process primary produces glycosidic bond cleavages named $Y_n$, $C_n$, $B_n$ and $Z_n$, according to Domon and Costello nomenclature,[42] n representing the number of rings retained in the structure. $Y_n$ and $Z_n$ fragments correspond to the reducing end of a carbohydrate with the glycosidic oxygen ($Y_n$) and without the glycosidic oxygen ($Z_n$) respectively. Likewise, $C_n$ and $B_n$ fragment ions refer to the non-reducing end of a carbohydrate with and without the glycosidic oxygen respectively. Y, C, B and Z fragmentation patterns are shown in Scheme 2. Cross-ring fragments are also observed in the case of disaccharides; cross-ring fragments retaining the reducing end are named $^{i,j}A_n$ and cross-ring fragments retaining the non-reducing end are named $^{i,j}X_n$. The superscript "$i,j$" indicates carbons after which cleavages occur. In the present experiment all fragment ions are lithiated and the notation Y/C indicates ions that are either Y or C fragments (likewise for B/Z).

### Experimental collision cross sections

The total time required for an ion to traverse through the instrument is equivalent to the sum of the drift time, flight time, and the time required to travel through the instrument's interface regions. For a uniform electric field applied along the drift region, collision cross sections can be calculated directly

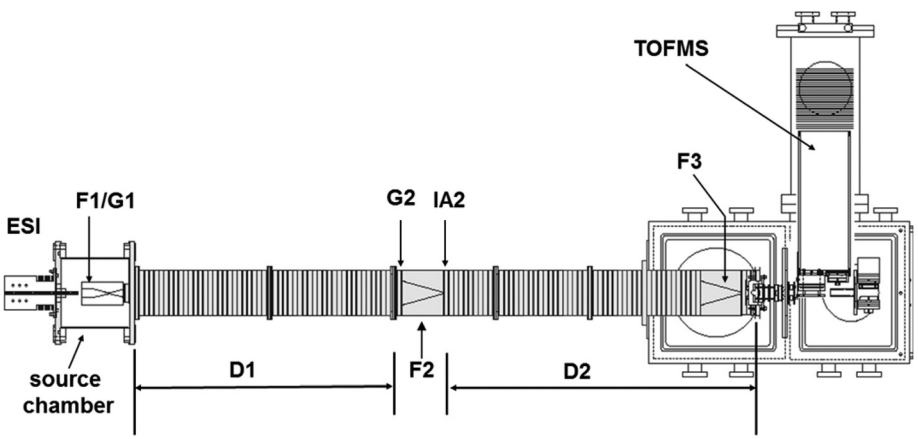


Fig. 1 Schematic diagram of the ion mobility/time-of-flight instrument. The primary instruments component are shown as well as the drift tube (D), ion funnels (F), ion gates (G) and the ion activation region (IA2).

 

Table 1 Measured collision cross-section for the studied carbohydrates

| | | | Collision cross section ($A^2$) | | | |
|---|---|---|---|---|---|---|
| Name | Constituents[a] | Linkage type[b] | $[M + Li]^+$ $m/z$ 511 | $[Y_2/c_2 + Li]^+$ $m/z$ 349 | $[B_2/Z_2 + Li]^+$ $m/z$ 331 | $[Y_1/C_1 + Li]^+$ $m/z$ 187 |
| Raffinose | Gla-Glc-Fruc | α 1-6, β 1-2 | 13704 | 120.3 | 118.5 | 102.9/104.1 |
| Melezitose | Glc-Fruc-Glc | α 1-2, α 1-2 | 132.6 | 115.6 | 113.2 | 100.7 |
| Maltotriose | Glc-Glc-Glc | α 1.4, α 1.4 | 138 | (116.7) 120.3 | 118 | na |
| | | | $[M + Li]^+$ $m/z$ 349 | $[M-H_2O + Li]^+$ $m/z$ 331 | $[Y_2/C_1 + Li]^+$ $m/z$ 187 | $[B_1/Z_1 + Li]^+$ $m/z$ 169 |
| Sucrose | Glc-Fruc | α 1-2 | 104.5 | na | 89.5 | 86.5 |
| Leucrose | Glu-Fruc | α 1-5 | 104.6 | Low intensity | 88 | (86.3) 88.7 |
| Palatinose | Glu-Fruc | α 1-6 | 106.4 | 105.6 | (85.4) 89.7 | 87.3 |
| Trehalose | Glc-Glc | α 1-1 | 105.1 | na | 90.3 | (87.3) 89.2 |
| Cellobiose | Glc-Glc | β 1-4 | 108.6 | 105.7 | 91.4 | 87/88.8 |
| β-Gentiobiose | Glc-Glc | β 1-6 | 108.1 | 105.7 (108.2) | 91.7 | 87 (90) |
| Isomaltose | Glc-Glc | α 1-6 | 108.6 | Low intensity | 91.9 | Low intesnity |
| Maltose | Glc-Glc | α 1-4 | 110.6 | Low intensity | 92.7 | (89.2) 91 |
| Lactose | Glc-Glc | β 1-4 | 103 | 102.3 | 88.9 | 86 |
| Melibiose | Glc-Glc | α 1-2 | 107.4 | Low intensity | 92.1 | 88.6 (91) |
| | | | | | $[M + Li]^+$ $m/z$ 187 | |
| Glucose | Glc | | | | 80.8 (92.3) | |
| Galactose | Gal | | | | 76.3/78.1 (90.3) | |
| Fructose | Fruc | | | | 77.5/78.7 (90.3) | |

[a] Monosaccharide units for the studied carbohydrates are galactose (Gal), glucose (Glc) and fructose (Fruc). [b] Refers to the linkage between two monosaccharide units from the non-reducing end to the reducing end of the carbohydrate. na: The fragment ion was not observed. Low intensity: The intensity of the fragment ion was too low for a collisional cross-section to be measured. In the case of multiple features, the ccs for the least intense feature is indicated in parenthesis; ccs for two peaks of equal intensities are separated by a forward slash.

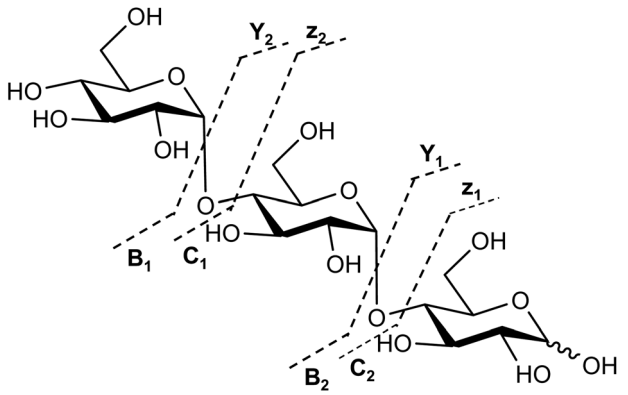


Scheme 2 Types of fragment ions shown on the trisaccharide maltotriose.

from the drift time distributions (through the entire instrument) using eqn (1),[43]

$$\Omega = \frac{(18\pi)^{1/2}}{16}\frac{ze}{(k_b T)^{1/2}}\left[\frac{1}{m_I}+\frac{1}{m_B}\right]^{1/2}\frac{t_D E}{L}\frac{760}{P}\frac{T}{273.2}\frac{1}{N}, \quad (1)$$

where ze, $k_b$, $m_I$, and $m_B$ refer to the charge of the ion, Boltzmann's constant, the mass of the ion, and the mass of the buffer gas (helium in these experiments). The variables $t_D$, $E$, $L$, $P$, $T$, and $N$ correspond to the drift time, electric field, drift tube length, buffer gas pressure and temperature, and the neutral number density of the buffer gas, respectively. The final term in the equation normalizes the mobility to standard temperature and pressure (STP). Due to the presence of the two funnels at F2 and F3 which are operated at a relatively high field, cross section determination through the entire instrument often involves a simple calibration technique for which the individual drift times for well-characterized ions (typically bradykinin and polyalanine) are used for calibration. The calibration can be tested using a highly rigorous approach for determining cross sections involving scanning across a peak by varying the application time of the gates G1 and G2. The delay time applied at G2 in order to select a specific precursor ion defines its drift time. The conversion to cross sections of selected ions is then accomplished with no additional corrections through eqn (1) using the appropriate drift lengths. Similarly the cross sections of fragment ions can be determined through the second drift region.

## Results and discussion

### IMS-CID-IMS-MS analyses of lithiated carbohydrates

An example spectrum resulting from an IMS-CID-IMS-MS experiment performed on the trisaccharide melezitose is shown in Fig. 2. Ions are observed over a range of $m/z$ and drift time values: from 169 $m/z$ to 511 $m/z$; and, from 9.9 ms to

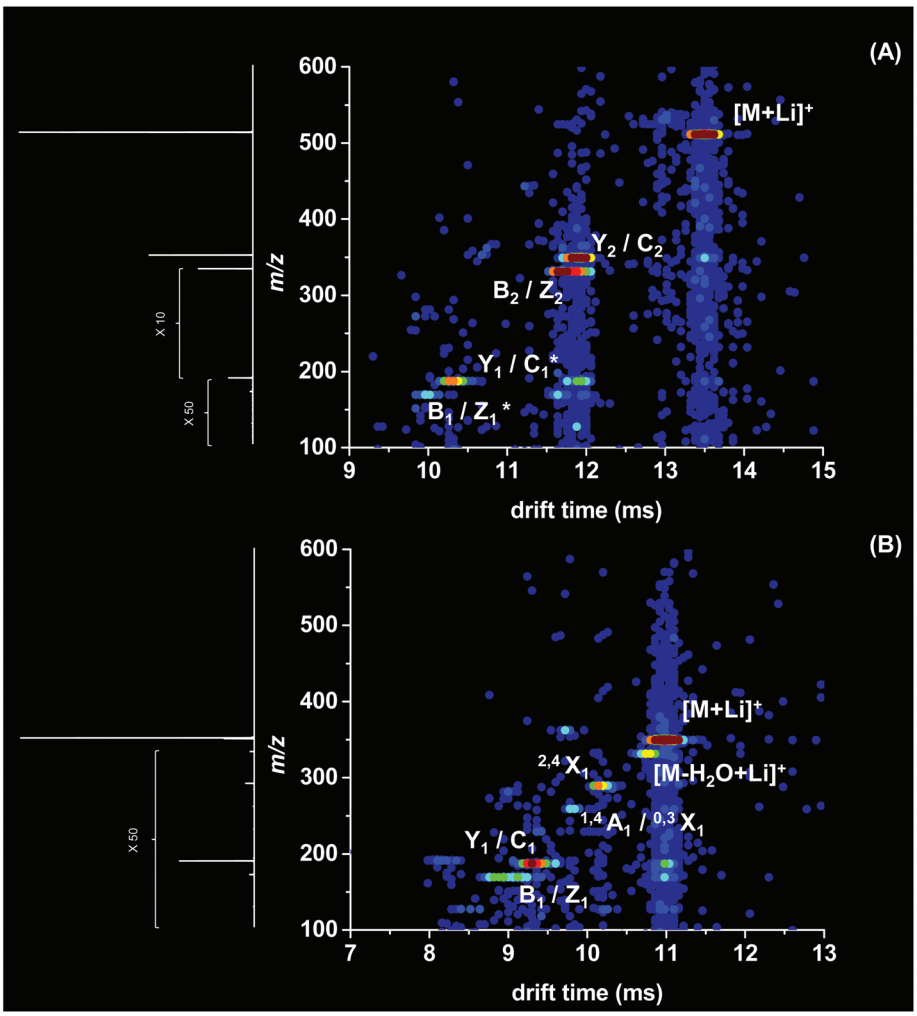


**Fig. 2** Two-dimensional nested IMS-MS dot plots (ion intensity as a function of drift time and *m/z* values) obtained for the fragmentation of lithiated melezitose (A) and lithiated β-gentiobiose (B). The corresponding mass spectra are shown as an insert on the left side. Features corresponding to precursor ions (M) and fragment ions ($Y_2/C_2$, $B_2/Z_2$, $Y_1/C_1$, $B_1/Z_1$, $^{2,4}X_1$ and $^{1,4}A_1/^{0,3}X_1$) are indicated. In the case of melezitose (A) $Y_1/C_1^*$ and $B_1/Z_1^*$ indicate the existence of additional fragment assignments – originating from breaking two glycosidic bonds simultaneously to yield the monosaccharide unit in the middle of the trisaccharide sequence – for the given feature. $Y_2$–$Z_1/C_2$–$B_1$ are isobaric of $Y_1/C_1$; $B_2$–$B_1/Z_2$–$Z_1$ and $Y_2$–$Y_1/C_2$–$C_1$ are isobaric of $B_1/Z_1$.

13.5 ms in the drift time dimension. The precursor ion $[M + Li]^+$ at 511 *m/z* is the most intense feature. The most intense fragments are $Y_2/C_2$ and $B_2/Z_2$ at respectively 349 *m/z* and 331 *m/z* with associated drift times of 11.9 ms and 11.8 ms. Both $Y_2/C_2$ and $B_2/Z_2$ fragments correspond to the loss of one monosaccharide unit by glycosidic bond cleavage. A loss of a disaccharide by cleaving one of the two glycosidic bonds gives rise to peaks at 187 *m/z* ($t_D$ = 10.3 ms) and 169 *m/z* ($t_D$ = 9.9 ms). Finally, the feature at 187 *m/z* with an associated drift time of 12 ms (Fig. 2) is the consequence of the fragmentation of the $Y_2/C_2$ ion in the back of our home-built instrument (Fig. 1). This feature is clearly resolved in the mobility dimension from the isobaric fragment $Y_1/C_1^*$ (187 *m/z*, $t_D$ = 10.3 ms) generated in the instrument mid funnel (F2). The star symbol on $Y_1/C_1^*$ indicates the possibility of an additional fragment assignment ($Y_2$–$Z_1/C_2$–$B_1$ isobaric of $Y_1/C_1$), originating from breaking two glycosidic bonds simultaneously to yield the monosaccharide unit in the middle of the trisaccharide sequence.

In the case of the disaccharide β-gentiobiose, fragments resulting from both glycosidic bond cleavage and cross-ring fragments are produced. Fig. 2 illustrates the 2D-plot and associated mass spectrum resulting from the IMS-CID-IMS-MS experiment completed on β-gentiobiose. The precursor ion $[M + Li]^+$ (349 *m/z*, $t_D$ = 11 ms) is the feature with the largest intensity in both the 2D-plot and the mass spectrum (Fig. 2). The main fragment resulted from glycosidic bond cleavage with retention of the glycosidic oxygen ($Y_1/C_1$, 187 *m/z*, $t_D$ = 9.3 ms). The $Y_1/C_1$ fragment ion originating from β-gentiobiose is representative of one monosaccharide unit and interestingly the structure obtained here has a shorter drift time (1 ms difference) than the corresponding isobaric fragment ion obtained from the trisaccharide melezitose. Similarly, the fragment ion

 

resulting from glycosidic cleavage without retention of the glycosidic oxygen ($B_1/Z_1$, 169 $m/z$) appeared at a shorter time ($t_D$ = 9 ms) than its counterpart ($t_D$ = 9.9 ms) resulting from melezitose fragmentation. In the case of melezitose and β-gentiobiose, both $Y_1/C_1$ and $B_1/Z_1$ fragments are made of a glucose unit but differ by the type of glycosidic linkage that was broken (α 1–2 and β1–6 respectively). The fact that isobaric fragments resulting from β-gentiobiose or melezitose have different drift times suggests that these two fragments retained linkage information form the precursor ion, resulting in different structure(s) and/or conformer(s). Thus, population of fragment ions are used to distinguish carbohydrate isomers. Structural similarities and differences between fragment ions are further investigated by examining their corresponding mobility profiles. Additional fragments are reported (Fig. 2): $[M - H_2O + Li]^+$ resulting from the loss of water (331 $m/z$, $t_D$ = 10.7 ms) as well as cross-ring fragments $^{2,4}X_1$ (289 $m/z$, $t_D$ = 10.1 ms) and $^{1,4}A_1/^{0,3}X_1$ (259 $m/z$, $t_D$ = 9.8 ms). Lastly, fragment ions with an associated drift time of 11 ms (Fig. 2, 169 $m/z$ and 187 $m/z$) resulting from fragmentation in the back of the instrument are resolved from the fragment ions of interest $Y_1/C_1$ ($t_D$ = 9.3 ms) and $B_1/Z_1$ (($t_D$ = 9 ms).

### Disaccharide mobility distributions for delineation between isomers

The mobility distribution of an ion is generated from the 2D-plot by integrating all $m/z$ bins (centered on the ion $m/z$) across a narrow range for each drift time bin. Collision cross sections (ccs in Å$^2$) are derived from the mobility equation as described elsewhere.[5,44] Fig. 3 depicts mobility profiles of lithiated disaccharide ions.

**Precursor ion $[M + Li]^+$ (349 $m/z$).** Maltose, β-gentiobiose, cellobiose and trehalose are isomers made of two glucoses that differ by only the type of glycosidic linkage (Table 1). Mobility distributions for maltose, β-gentiobiose and trehalose precursor ions display a single sharp feature. Interestingly, the mobility profile of cellobiose shows a broader feature. A similar trait is observed in the case of precursor ions lactose and melibiose. That is, the mobility distribution for lactose is broader than the mobility distribution of melibiose (data not shown). Both lactose and melibiose are made of galcatose and glucose, the former having a β 1–4 type of glycosidic linkage (α 1–6 for melibiose, Table 1). The observed broadening of the mobility feature for a disaccharide with a β 1–4 linkage type suggests that this type of linkage is likely to give rise to multiple conformations in the gas phase. An exhaustive study of the conformational space occupied by carbohydrate isomers is beyond the scope of this paper and will be addressed in the future by using annealing techniques such as IMS-IMS-MS. Cellobiose and β-gentiobiose precursor ions have similar ccs (respectively 108.6 Å$^2$ and 108.1 Å$^2$) and cannot be distinguished in the present case. In contrast, trehalose and maltose precursor ions have ccs, not only different from each other, but also different from cellobiose and β-gentiobiose. Trehalose is the most compact ion with a ccs centered at 105.1 Å$^2$ and maltose is the most elongated ion with a ccs centered at 110.6 Å$^2$. As result, the two isomers trehalose and maltose can be distinguished based on their respective mobility distributions.

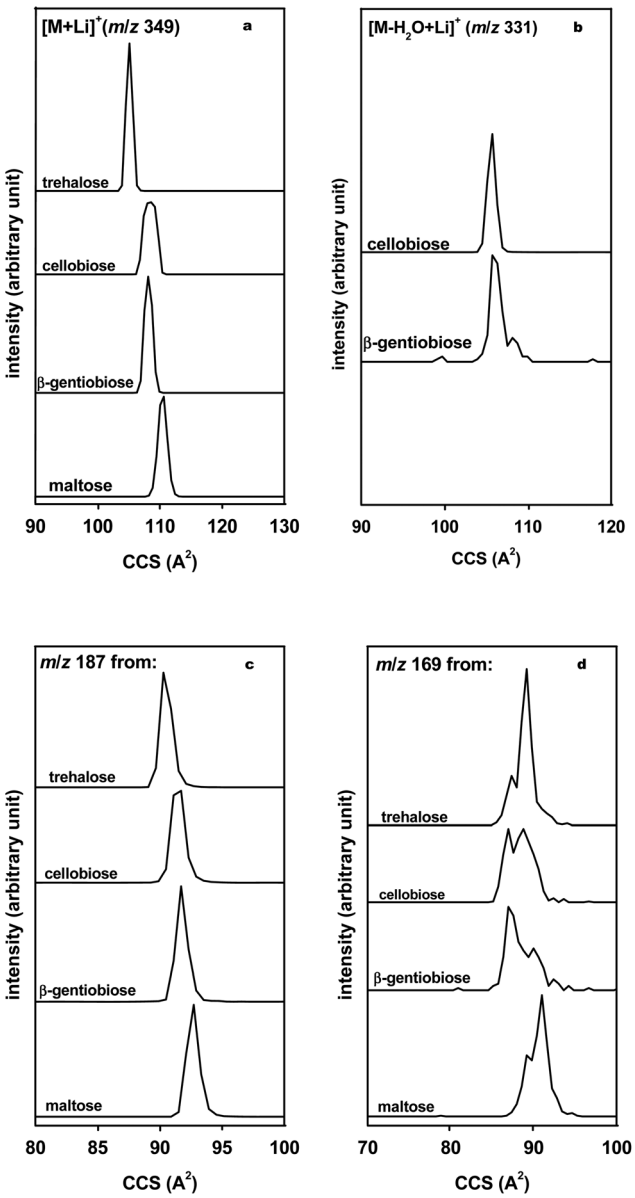


Fig. 3 Mobility distributions, on a collision cross section (ccs) scale, of lithiated glucose disaccharides obtained by IMS-MS (precursor ions) and lithiated fragment ions obtained by IMS-CID-IMS-MS. (a) Precursor ions trehalose, cellobiose, β-gentiobiose and maltose. (b) Fragment ions at $m/z$ 331 corresponding to the loss of water from the precursor ion for cellobiose and β-gentiobiose. (c) and (d) Fragment ions at respectively $m/z$ 187 ($Y_1/C_1$) and 169 ($B_1/Z_1$) resulting from the glycosidic bond cleavage between the two glucose units of trehalose, cellobiose, β-gentiobiose and maltose.

Mobility distributions for ions resulting from the neutral loss of a water molecule from the precursor ion after being subjected to IMS-CID-IMS-MS ($[M - H_2O + Li]^+$, $m/z$ 331) are depicted for cellobiose and trehalose (Fig. 3). This ion was not observed after fragmentation of the precursor ion trehalose

and was of very low intensity for the precursor ion maltose. The mobility distribution of $[M - H_2O + Li]^+$ originating from cellobiose displays a single feature at 105.7 Å$^2$. Interestingly, the mobility distribution of $[M - H_2O + Li]^+$ arising from β-gentiobiose displays multiple features: the main feature is centered at 105.7 Å$^2$, two shoulders at 108.2 Å$^2$ and 110.0 Å$^2$ and one more compact feature at 98.7 Å$^2$. The features at 105.7 Å$^2$, 108.2 Å$^2$ and 110.0 Å$^2$ most likely result from different conformers of this fragment. The peak at 98.7 Å$^2$ could result from a neutral loss of water at an alternate location of the carbohydrate, and as a result an additional structure of this ion in the gas phase is observed.

**Fragment ions with retention of the glycosidic oxygen.** Mobility profiles of fragments $Y_1/C_1$ (*m*/*z* 187) originating from glucose-only disaccharides (Fig. 3) present a trend similar to the one observed for the precursor ions. It is interesting to note that the mobility distribution of fragment ions are broader than in the case of precursor ions. A possible explanation of this phenomenon is that for a given *m*/*z*, the charge carried by the lithium atom is either retained by the reducing end (Y fragment) or retained by the non-reducing end (C fragment), hence yielding a greater number of possible conformers than for the corresponding precursor ion. The delineation between isobaric Y and C fragment ions will allow unambiguous sequencing of carbohydrate isomers and is currently investigated by our group.

**Fragment ions without the glycosidic oxygen.** $B_1/Z_1$ fragments (*m*/*z* 169, Fig. 3) originating from glucose disaccharides isomers have unique mobility distributions comprised of multiple features. The fragment ion resulting from the IMS-CID-IMS-MS experiment performed on maltose (*m*/*z* 169, Fig. 3, bottom trace) displays two main features at respectively 89.2 Å$^2$ and 91.0 Å$^2$, the latter being greater in intensity; and a minor elongated feature centered at 94.6 Å$^2$. In the case of fragment originating from β-gentiobiose (Fig. 3, second trace from bottom), the most compact feature (86.7 Å$^2$) is greater in intensity than the more elongated one (90.0 Å$^2$); additionally, two minor features at 92.4 Å$^2$ and 94.2 Å$^2$ are present. Similar minor features (92.4 Å$^2$ and 93.6 Å2) are also visible on the mobility distribution of the $B_1/Z_1$ fragment originating from cellobiose (Fig. 3, second trace from top); the two main features (87.0 Å$^2$ and 88.8 Å$^2$) are of equal intensities. Finally, fragment originating from trehalose (Fig. 3, top trace) generated a mobility profile with a compact feature at 87.3 Å$^2$, a more elongated feature at 89.2 Å$^2$ with an intensity ~2.5 greater than the compact one and a minor feature at 94 Å$^2$. Collision cross sections for the main features of B/Z fragment ions initiated by trehalose and cellobiose are close but the relative intensities in which these features exist are drastically different. For this reason, trehalose and cellobiose isomers can be distinguished based on the mobility distributions of their respective B/Z fragment ions. B and Z fragment ions are oxonium ions formed respectively at the reducing end of a carbohydrate (B fragment) or the non-reducing end of a carbohydrate (Z fragment).[36] These two different structures most likely generated different conformations or population of conformations upon binding to a lithium atom. As a consequence, the two main features observed in the four disaccharide fragments could be respectively representative of B and Z ions. Further studies are underway to distinguish B and Z ions.

**Glucose-fructose disaccharides.** Mobility profiles associated with sucrose, leucrose and palatinose, which differ only by the type of glycosidic bond, are depicted in Fig. 4. All three pre-

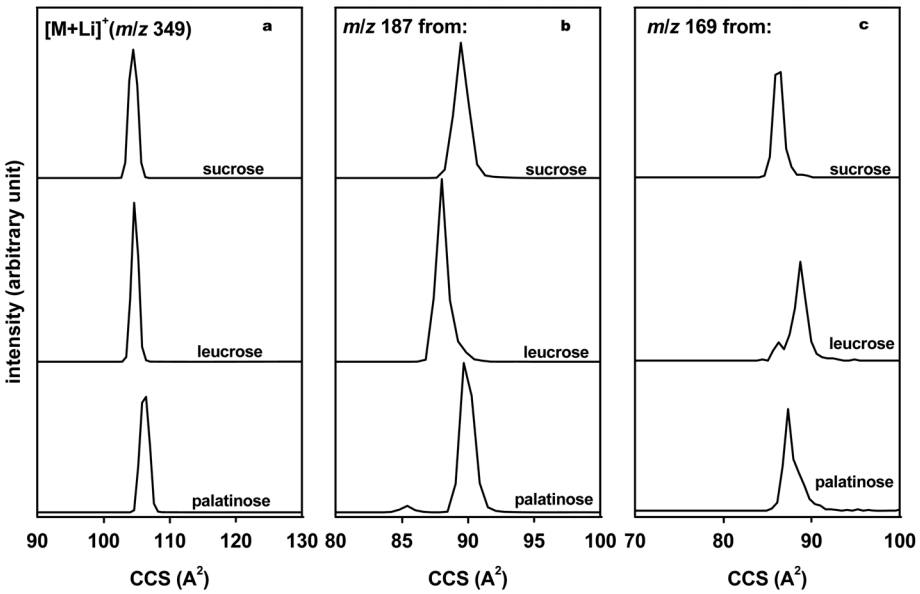


Fig. 4 Mobility distributions of lithiated sucrose (top trace), leucrose (middle trace) and palatinose (bottom trace). (a) Precursor ions $[M + Li]^+$ (*m*/*z* 349) are obtained by IMS-MS. (b) and (c) Lithiated fragment ions obtained by IMS-CID-IMS-MS (*m*/*z* 187 and *m*/*z* 169).

 

cursor ions $[M + Li]^+$ ($m/z$ 349) display a single sharp feature. Sucrose and leucrose have similar ccs (104.5 Å$^2$ and 104.6 Å$^2$, respectively) while palatinose has a larger structure (106.4 Å$^2$). Interestingly, mobility distributions of $Y_1/C_1$ fragment ions ($m/z$ 187, Fig. 4) are different for all three isomers. The fragmentation of palatinose (Fig. 4, bottom trace) yielded two features; a compact (low intensity) feature with an associated ccs of 85.4 Å$^2$ and a more elongated one at 89.7 Å$^2$. The mobility distribution of the $Y_1/C_1$ fragment originating from sucrose displays a single peak centered at 89.5 Å$^2$ (Fig. 4, top trace). Although the ccs value associated with fructose fragment ion is close to the one measured for the main feature of the palatinose $Y_1/C_1$ ion, the two ions can be distinguished because the fragmentation of palatinose generated an additional conformation or ensemble of conformations (85.4 Å$^2$, Fig. 4, bottom trace) not observed when sucrose is fragmented. The mobility profile of the $Y_1/C_1$ fragment ion obtained from leucrose presents a single feature (88.0 Å$^2$, Fig. 4, middle trace) and is distinct from the two other fragment ion mobility profiles.

The delineation between sucrose, leucrose and palatinose is further improved when the mobility distribution of $B_1/Z_1$ fragment ions are considered ($m/z$ 169, Fig. 4). The main peak originating from the fragmentation of sucrose is saturated ($m/z$ 169, 86.5 Å$^2$, Fig. 4, top trace). That is, sucrose fragmentation upon IMS-CID-IMS-MS was more efficient (yielded more intense features) in comparison with leucrose, palatinose and the other disaccharides examined in the present work. In addition a very low intensity feature is observed at 88.9 Å$^2$. The mobility distribution of the $B_1/Z_1$ ion initiated by leucrose fragmentation ($m/z$ 169, Fig. 4, middle trace) displays two features at respectively 86.3 Å$^2$ and 88.7 Å$^2$; the most elongated one being three times higher in intensity than the more compact one. Lastly, the $B_1/Z_1$ fragment ion originating from palatinose ($m/z$ 169, Fig. 4, bottom trace) shows a broad distribution centered at 87.3 Å$^2$ and an unresolved shoulder at ~89 Å$^2$. Interestingly, the population of ions observed at ~89 Å$^2$ in the case of $B_1/Z_1$ fragment ion yielded by palatinose is also observed in the case of leucrose (88.7 Å$^2$) and sucrose (88.9 Å$^2$); this population of ions is likely to be specific to either B or Z ions. As we discussed above for glucose disaccharide isomers, multiple features observed on the mobility profiles of $B_1/Z_1$ fragment ions are likely to be representative of unique population of conformers for B and Z fragment ions respectively. In summary, sucrose, leucrose and palatinose isomers are unambiguously distinguished based on the mobility distribution of their respective fragment ions generated by IMS-CID-IMS-MS.

### Mobility distributions of trisaccharide isomers

Mobility profiles of raffinose, melezitose and maltotriose precursor ions $[M + Li]^+$ ($m/z$ 511) are depicted in Fig. 5. The mobility distribution of melezitose precursor ion (Fig. 5) displays a unique feature centered at 132.6 Å$^2$ which can be differentiated from the single feature in mobility profiles of both raffinose (137.4 Å$^2$) and maltotriose (138.0 Å$^2$) precursor ions. The middle panel of Fig. 5 illustrates mobility distributions of $Y_2/C_2$ fragment ions ($m/z$ 349) obtained by IMS-CID-IMS-MS analysis of raffinose, melezitose and maltotriose precursor ions. Interestingly, the mobility profile of the $Y_2/C_2$ fragment ion, originating from maltotriose fragmentation ($m/z$ 349, Fig. 5, bottom trace), shows two features. The main feature has an associated ccs of 120.3 Å$^2$, and the more compact feature (approximately ten times lower in intensity) has a ccs centered at 116.7 Å$^2$. Because the $Y_2/C_2$ ion generated by the fragmentation of raffinose ($m/z$ 349, Fig. 5, top trace) presents a single

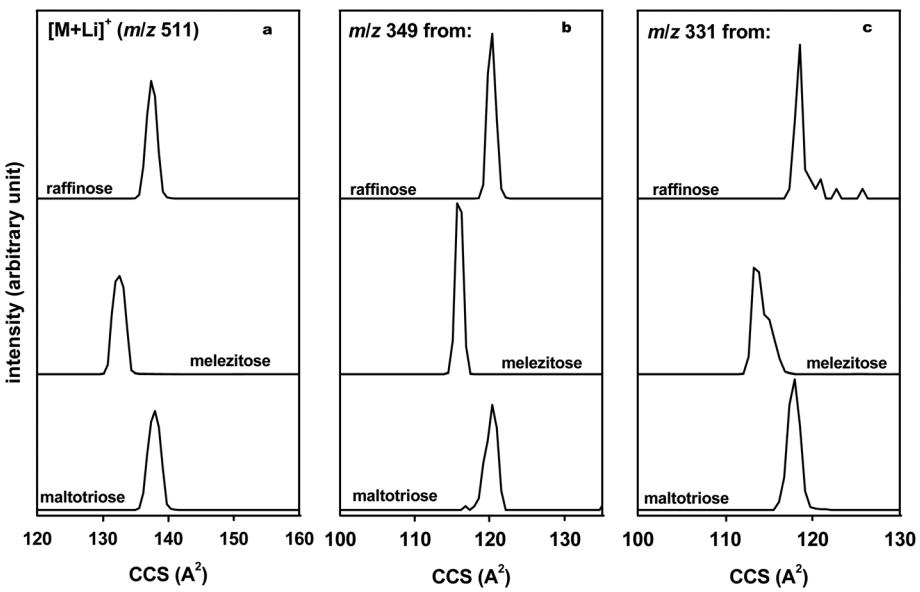


Fig. 5 Mobility distributions of trisaccharides raffinose (top trace), melezitose (middle trace) and maltotriose (bottom trace). (a) Precursor ions ($m/z$ 511) are obtained by IMS-MS. (b) and (c) Fragment ions are obtained by IMS-CID-IMS-MS ($m/z$ 349 and $m/z$ 331). All species are lithiated.

feature at 120.3 Å$^2$, raffinose and maltotriose can be distinguished in the present case. Melezitose $Y_2/C_2$ fragment ion has a more compact structure (*m*/*z* 349, 115.6 Å$^2$, Fig. 5, middle trace) than the structures obtained for fragment ions originating from raffinose and maltotriose.

As observed for disaccharide precursor ions, the mobility distribution of B/Z fragment ions often show shoulders on the main peak. The most compact structure is obtained for the $B_2/Z_2$ fragment initiated by melezitose (*m*/*z* 331, Fig. 5, middle trace); a broad distribution centered at 113.3 Å$^2$ and a shoulder at ~115 Å$^2$. The mobility distribution of the $B_2/Z_2$ ion originating from the fragmentation of raffinose displays multiple features (*m*/*z* 331, Fig. 5, top trace); a main feature (118.5 Å$^2$) and three minor features (120.9 Å$^2$, 122.7 Å$^2$ and 125.7 Å$^2$). Lastly, the mobility distribution of $B_2/Z_2$ ions arising from the fragmentation of maltotriose (*m*/*z* 331, Fig. 5, bottom trace) shows a single feature with an associated ccs of 118.0 Å$^2$; interestingly, there are no minor features, and therefore can be distinguished from the $B_2/Z_2$ ions originating from raffinose.

### Using complementary IMS fragment ion information to characterize precursor ion isomers

Recently, Eyers and coworkers have described the idea of using IMS information to complement MS-based sequencing methods.[36] The basic idea of this approach is that fragments containing specific residues and linkages cannot be unambiguously identified based on MS information alone; however, these fragments once formed retain elements of structure that are specific to different isomers. Thus, information about their respective mobilities can be used to discriminate between species having identical masses. Our data indicates a similar trend. Fig. 6 depicts ccs for ten disaccharide precursor ions plotted as a function of ccs for $Y_1/C_1$ and $B_1/Z_1$ fragment ions. Lactose, palatinose and maltose are unambiguously distinguished based on the precursor ion ccs alone (along the *x*-axis, Fig. 6). Sucrose, leucrose and trehalose (similarly melibiose, β-gentiobiose, isomaltose and cellobiose), which cannot be separated based on ccs of their respective precursor ions, are unequivocally distinguished when ccs for fragment ions are taken into account (along the *y*-axis, Fig. 6).

In addition, the identity of the fragment monomeric unit (glucose, galactose or fructose) as well as the type of fragment ion are represented (Fig. 6). Unlike previous studies, we examine here the fragmentation of carbohydrate isomers yielding isobaric Y/C and B/Z fragment ions. Because of this, an ambiguity remains for the comprehensive characterization of the carbohydrate building blocks. For example, the data point representing the $Y_1$ (or $C_1$) fragment arising from sucrose (Fig. 6) can either be a glucose or a fructose unit (and reciprocally). Because this data point belongs to a cluster of reported values for the ccs distribution of $Y_1/C_1$ fragment of disaccharides made of glucose only, extending on a diagonal from trehalose to maltose, it can be inferred that the obtained $Y_1/C_1$ fragment from sucrose is most likely the glucose fragment (C1). In a similar fashion, the localization of the data point for the C1/Y1 fragment arising from leucrose could be indicative

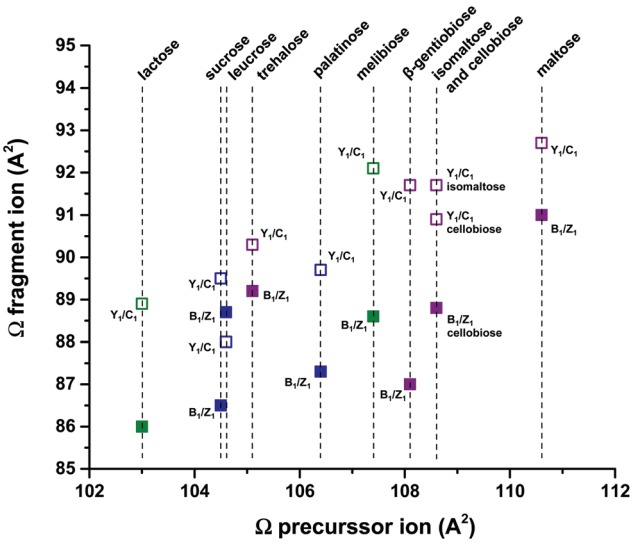


Fig. 6 Collision cross section (ccs) of lithiated disaccharide precursor ions as a function of the ccs of $Y_1/C_1$ (empty squares) and $B_1/Z_1$ (full squares) lithiated fragment ions (in the case of multiple peaks, the main feature is reported). Dash lines indicate the position of the precursor ion ccs in a single dimension (*x*-axis). The nature of the monosaccharide fragment unit is represented by a color code: glucose in purple, glucose or fructose in blue and glucose or galactose in green.

of the presence of a fructose unit, as this data point is situated outside the observed trend for glucose units. Overall, the combination of precursor- and fragment ions ccs measurements, not only allow delineation between carbohydrate isomers, but also shows potential as a high-throughput sequencing methodology, which will be permitted by the structural characterization of monomeric building blocks.

## Summary and conclusions

Lithiated oligosaccharides were examined using IMS-MS and IMS-CID-IMS-MS. In favorable cases, carbohydrate isomers can be distinguished based only on the mobility distribution of the singly-lithiated precursor ion. Trehalose, maltose, melibiose, lactose and melezitose are such isomers. Otherwise, a different approach is necessary. The present work demonstrates that the mobility distribution of lithiated fragment ions obtained by IMS-CID-IMS-MS can be used to distinguish between underivatized carbohydrate isomers. The main fragments obtained when CID is performed in the drift tube originate from the cleavage of a glycosidic bond (Y/C and B/Z fragments). In most cases, the mobility profile of a fragment ion display multiple features. This set of features is unique for a given precursor ion. That is, one feature exists for one precursor ion but not the other, or if the same features are present (*i.e.*, at similar ccs), their relative abundances vary from one isomer to another. In other words, different carbohydrate isomers generate fragment ions characterized by different population of conformers and/or structures. CCSs measured in

 

He buffer gas of carbohydrate precursor and fragment ions for three monosaccharide isomers, ten disaccharide isomers and three trisaccharide isomers are reported. In addition, broader features were observed for fragment ions in comparison with corresponding precursor ions. A probable explanation for this trend is that when a glycosidic bond is broken, (1) the charge is carried by either the reducing end (Y, Z fragments) or the non-reducing end (C, B fragments) of the carbohydrate; and (2) for each type of fragment, the multiple possible locations at which the lithium atom binds are likely to generate multiple conformations. Thus, broader features, which are observed in mobility profiles of fragment ions, are most likely comprised of multiple structures and/or conformers. We are currently investigating means to better resolve these distributions in order to delineate between isobaric Y and C (similarly B and Z) fragment ions. This methodology, in combination with a concerted effort for building a ccs library of precursor- and fragment-ions, holds potential for high-throughput sequencing of linear carbohydrates.

## Acknowledgements

This work is supported by the National Institute of Health (NIH-5R01GM93322-2).

## References

1 R. A. Laine, Information capacity of the carbohydrate code, *Pure Appl. Chem.*, 1997, **69**(9), 1867–1873.
2 C. Sansom and O. Markman, *Glycobiology*, Scion Publishing Ltd, 2007.
3 *Essentials of Glycobiology*, ed. A. Varki, R. Cummings, J. Esko, H. Freeze, G. Hart and J. Marth, CSHL Press, 2nd edn, 2009.
4 *Structural Glycobiology*, ed. E. Yuriev and P. A. Ramsland, CRC Press, 2013.
5 D. E. Clemmer and M. F. Jarrold, Ion Mobility Measurements and their Applications to Clusters and Biomolecules, *J. Mass Spectrom.*, 1997, **32**, 577–592.
6 C. S. Hoaglund, S. J. Valentine, C. R. Sporleder, J. P. Reilly and D. E. Clemmer, Three-Dimensional Ion Mobility/TOFMS Analysis of Electrosprayed Biomolecules, *Anal. Chem.*, 1998, **70**, 2236–2242.
7 W. R. Alley and M. V. Novotny, Structural Glycomic Analyses at High Sensitivity: A Decade of Progress, *Ann. Rev. Anal. Chem.*, 2013, **6**, 237–265.
8 L. R. Ruhaak, A. M. Deelder and M. Wuhrer, Oligosaccharide analysis by graphitized carbon liquid chromatography-mass spectrometry, *Anal. Bioanal. Chem.*, 2009, **394**(1), 163–174.
9 J. Jiao, H. Zhang and V. N. Reinhold, High performance IT-MS$^n$ sequencing of glycans: Spatial resolution of ovalbumin isomers, *Int. J. Mass Spectrom.*, 2011, **303**(2–3), 109–117.
10 S. Mittermayr, J. Bones and A. Guttman, Unraveling the Glyco-Puzzle: Glycan Structure Identification by Capillary Electrophoresis, *Anal. Chem.*, 2013, **85**(9), 4228–4238.
11 J. M. Prien, D. J. Ashline, A. J. Lapadula, H. Zhang and V. N. Reinhold, The high mannose glycans from bovine ribonuclease B isomer characterization by ion trap MS, *J. Am. Soc. Mass Spectrom.*, 2009, **20**, 539–556.
12 E. V. Da Costa, A. S. P. Moreira, F. M. Nunes, M. A. Coimbra, D. V. Evtuguin and M. R. M. Domingues, Differentiation of isomeric pentose disaccharides by electrospray ionization tandem mass spectrometry and discriminant analysis, *Rapid Commun. Mass Spectrom.*, 2012, **26**(24), 2897–2904.
13 J. T. Adamson and K. Hakansson, Electron Capture Dissociation of Oligosaccharides Ionized with Alkali, Alkaline Earth, and Transition Metals, *Anal. Chem.*, 2007, **79**, 2901–2910.
14 X. Yu, Y. Q. Huang, C. Lin and C. E. Costello, Energy-Dependent Electron Activated Dissociation of Metal-Adducted Permethylated Oligosaccharides, *Anal. Chem.*, 2012, **84**(17), 7487–7494.
15 W. R. Alley Jr., Y. Mechref and M. V. Novotny, Characterization of glycopeptides by combining collision-induced dissociation and electron-transfer dissociation mass spectrometry data, *Rapid Commun. Mass Spectrom.*, 2009, **23**(1), 161–170.
16 L. Han and C. Costello, Electron Transfer Dissociation of Milk Oligosaccharides, *J. Am. Soc. Mass Spectrom.*, 2011, **22**(6), 997–1013.
17 A. Devakumar, M. S. Thompson and J. P. Reilly, Fragmentation of oligosaccharide ions with 157 nm vacuum ultraviolet light, *Rapid Commun. Mass Spectrom.*, 2005, **19**, 2313–2320.
18 J. J. Wilson and J. S. Brodbelt, Ultraviolet photodissociation at 355 nm of fluorescently labeled oligosaccharides, *Anal. Chem.*, 2008, **80**, 5186–5196.
19 S. Lee, S. J. Valentine, J. P. Reilly and D. E. Clemmer, Analyzing a Mixture of Disaccharides by IMS–VUVPD–MS, *Int. J. Mass Spectrom.*, 2012, **309**, 161–167.
20 M. Zhu, B. Bendiak, B. Clowers and H. H. Hill Jr., Ion mobility-mass spectrometry analysis of isomeric carbohydrate precursor ions, *Anal. Bioanal. Chem.*, 2009, **394**(7), 1853–1867.
21 K. F. Aoki-Kinoshita, *Glycome Informatics*, CRC Press, Taylor & Francis Group, 2010.
22 Y. Liu and D. E. Clemmer, Characterizing Oligosaccharides Using Injected–Ion Mobility/Mass Spectrometry, *Anal. Chem.*, 1997, **69**, 2504–2509.
23 D. Isailovic, R. T. Kurulugama, M. D. Plasencia, S. T. Stokes, Z. Kyselova, R. Goldman, Y. Mechref, M. V. Novotny and D. E. Clemmer, Profiling of human serum glycans associated with liver cancer and cirrhosis by IMS-MS, *J. Proteome Res.*, 2008, **7**, 1109–1117.
24 M. D. Plasencia, D. Isailovic, S. I. Merenbloom, Y. Mechref and D. E. Clemmer, Resolving and Assigning N-linked

Glycan Structural Isomers from Ovalbumin by IMS-MS, *J. Am. Soc. Mass Spectrom.*, 2008, **19**(11), 1706–1715.

25 S. M. Zucker, S. Lee, N. Webber, S. J. Valentine, J. P. Reilly and D. E. Clemmer, An Ion Mobility/Ion Trap/Photodissociation Instrument for Characterization of Ion Structure, *J. Am. Soc. Mass Spectrom.*, 2011, **22**, 1477–1485.

26 F. Zhu, S. Lee, S. J. Valentine, J. P. Reilly and D. E. Clemmer, Mannose7 Glycan Isomer Characterization by IMS-MS/MS Analysis, *J. Am. Soc. Mass Spectrom.*, 2012, **23**, 2158–2166.

27 S. Lee, T. Wyttenbach and M. T. Bowers, Gas phase structures of sodiated oligosaccharides by ion mobility ion chromatography methods, *Int. J. Mass Spectrom.*, 1997, **167**, 605–614.

28 B. H. Clowers, P. Dwivedi, W. E. Steiner, H. H. Hill Jr. and B. Bendiak, Separation of sodiated isobaric disaccharides and trisaccharides using electrospray ionization-atmospheric pressure ion mobility-time of flight mass spectrometry, *J. Am. Soc. Mass Spectrom.*, 2005, **16**(5), 660–669.

29 P. Dwivedi, B. Bendiak, B. H. Clowers and H. H. Hill Jr., Rapid resolution of carbohydrate isomers by electrospray ionization ambient pressure ion mobility spectrometry-time-of-flight mass spectrometry (ESI-APIMS-TOFMS), *J. Am. Soc. Mass Spectrom.*, 2007, **18**(7), 1163–1175.

30 M. Zhu, B. Bendiak, B. Clowers and H. H. Hill Jr., Ion mobility-mass spectrometry analysis of isomeric carbohydrate precursor ions, *Anal. Bioanal. Chem.*, 2009, **394**(7), 1853–1867.

31 J. P. Williams, M. Grabenauer, R. J. Holland, C. J. Carpenter, M. R. Wormald, K. Giles, D. J. Harvey, R. H. Bateman, J. H. Scrivens and M. T. Bowers, Characterization of simple isomeric oligosaccharides and the rapid separation of glycan mixtures by ion mobility mass spectrometry, *Int. J. Mass Spectrom.*, 2010, **298**(1–3), 119–127.

32 L. S. Fenn and J. A. McLean, Structural resolution of carbohydrate positional and structural isomers based on gas-phase ion mobility-mass spectrometry, *Phys. Chem. Chem. Phys.*, 2011, **13**(6), 2196–2205.

33 D. J. Harvey, C. A. Scarff, M. Edgeworth, M. Crispin, C. N. Scanlan, F. Sobott, S. Allman, K. Baruah, L. Pritchard and J. H. Scrivens, Travelling wave ion mobility and negative ion fragmentation for the structural determination of N-linked glycans, *Electrophoresis*, 2013, **34**(16), 2368–2378.

34 H. L. Li, B. Bendiak, W. F. Siems, D. R. Gang and H. H. Hill Jr., Carbohydrate Structure Characterization by Tandem Ion Mobility Mass Spectrometry $(IMMS)^2$, *Anal. Chem.*, 2013, **85**(5), 2760–2769.

35 Y. T. Huang and E. D. Dodds, Ion Mobility Studies of Carbohydrates as Group I Adducts: Isomer Specific Collisional Cross Section Dependence on Metal Ion Radius, *Anal. Chem.*, 2013, **85**(20), 9728–9635.

36 P. Both, A. P. Green, C. J. Gray, R. Šardzík, J. Voglmeir, C. Fontana, M. Austeri, M. Rejzek, D. Richardson, R. A. Field, G. Widmalm, S. L. Flitsch and C. E. Eyers, Discrimination of epimeric glycans and glycopeptides using IM-MS and its potential for carbohydrate sequencing, *Nat. Chem.*, 2014, **6**, 65–74.

37 D. C. Collins and M. L. Lee, Developments in ion mobility spectrometry-mass spectrometry, *Anal. Bioanal. Chem.*, 2002, **372**(1), 66–73.

38 S. J. Valentine, Developing liquid chromatography ion mobility mass spectrometry techniques, *Expert Rev. Proteomics*, 2005, 553–565.

39 S. L. Koeniger, S. I. Merenbloom, S. J. Valentine, M. F. Jarrold, H. Udseth, R. Smith and D. E. Clemmer, An IMS-IMS Analogue of MS-MS, *Anal. Chem.*, 2006, **78**, 4161–4174.

40 S. I. Merenbloom, S. L. Koeniger, B. C. Bohrer, S. J. Valentine and D. E. Clemmer, Improving the Efficiency of IMS-IMS by a Combing Technique, *Anal. Chem.*, 2008, **80**(6), 1918–1927.

41 S. I. Merenbloom, S. L. Koeniger, S. J. Valentine, M. D. Plasencia and D. E. Clemmer, IMS–IMS and IMS–IMS–IMS/MS for Separating Peptide and Protein Fragment Ions, *Anal. Chem.*, 2006, **78**, 2802–2809.

42 B. Domon and C. E. Costello, A systematic nomenclature for carbohydrate fragmentations in FAB-MS MS spectra of glycoconjugates, *Glycoconjugate J.*, 1988, **5**(4), 397–409.

43 E. A. Mason and E. W. McDaniel, *Transport Properties of Ions in Gases*, Wiley, New York, 1988.

44 H. E. Revercomb and E. A. Mason, Theory of plasma chromatography/gaseous electrophoresis, Review, *Anal. Chem.*, 1975, **47**(7), 970–983.

 